Isothermal and Nonisothermal Reaction Kinetics in Solids: In Search of Ways toward Consensus

Sergey Vyazovkin and Charles A. Wight*

Department of Chemistry, University of Utah, Salt Lake City, Utah 84112

Received: June 10, 1997; In Final Form: August 21, 1997[⊗]

Thermogravimetric data for the decomposition of ammonium dinitramide (ADN) have been obtained under isothermal and nonisothermal conditions in order to determine the efficacy of different methods for analyzing the kinetics of solid-state reactions. A widely used model-fitting method gives excellent fits to the experimental data but yields highly uncertain values of the Arrhenius parameters when applied to nonisothermal data because temperature and extent of conversion are not independent variables. Therefore, comparison of model fitting results from isothermal and nonisothermal experiments is practically meaningless. Conversely, model-free isoconversional methods of kinetic analysis yield similar dependencies of the activation energy on the extent of conversion for isothermal and nonisothermal experiments. Analysis of synthetic data generated for a complex kinetic model suggests that, in the general case, the identical dependencies are unlikely to result from experiments obtained under isothermal and nonisothermal conditions.

Introduction

The concepts of solid-state kinetics were established[1−3] on the basis of experiments carried out under isothermal conditions. This was long before the first instruments for nonisothermal measurements became commercially available. Since then, the kinetic formalism has been extended to treat data obtained under nonisothermal conditions. The governing kinetic equation

$$d\alpha/dt = k(T)\, f(\alpha) \tag{1}$$

where t is the time and T is the temperature, makes the implicit assumption that the temperature dependence of the rate constant, $k(T)$, can be separated from the reaction model, $f(\alpha)$. Several examples of reaction models are given in Table 1. The extent of conversion, $0 \leqslant \alpha \leqslant 1$, is a global parameter typically evaluated from mass loss or reaction heat.

We may describe the explicit temperature dependence of the rate constant by replacing $k(T)$ with the Arrhenius equation, which gives

$$\frac{d\alpha}{dt} = A \exp\left(\frac{-E}{RT}\right) f(\alpha) \tag{2}$$

where A (the preexponential factor) and E (the activation energy) are Arrhenius parameters and R is the gas constant. Furthermore, for experiments in which samples are heated at a constant rate, the explicit time dependence of eq 2 can be eliminated through the trivial transformation

$$\frac{d\alpha}{dT} = \frac{A}{\beta} \exp\left(\frac{-E}{RT}\right) f(\alpha) \tag{3}$$

where $\beta = dT/dt$ is the heating rate.

The problem of interpretation of experimentally determined Arrhenius parameters is often associated with the problem of applicability of the Arrhenius equation in solid-state kinetics. The use of this equation has been criticized from a physical point of view.[4,5] Garn has stressed[5] that the Arrhenius equation is meaningfully applicable only to reactions that take place in an homogeneous environment. However, the Arrhenius equation has been quite successful in describing the temperature dependence of many thermally activated physical processes such nucleation and growth[6] or diffusion,[7] presumably because the system must overcome a potential energy barrier, and the energy distribution along the relevant coordinate is governed by Boltzmann statistics. Even for cases in which the density of available states is sparse, Galwey and Brown have shown[8] that Fermi−Dirac statistics (for electrons) and Bose−Einstein statistics (for phonons) also give rise to Arrhenius-like expressions. Therefore, the use of the Arrhenius equation is not only justifiable in terms of a rational parametrization, but also its use and physical interpretation are supported by a sound theoretical foundation.

Nevertheless, a practical problem of the interpretation of experimentally determined values of E and A does exist, and it lies in the very nature of the experiments.[9] The standard experimental techniques (e.g., TG, DSC, DTA) as well as more sophisticated methods[10,11] generally do not allow isolation of elementary reactions. Rather, they provide a global measure of the rate or extent of a process that usually involves several steps with different activation energies. For this reason, experimentally derived Arrhenius parameters of a solid-state process must be interpreted as effective values unless mechanistic conclusions can be justified by ancillary data.

Arrhenius parameters obtained from isothermal and nonisothermal data are often reported to be inconsistent. This caused McCallum and Tanner[12] to doubt the validity of eq 3 and to hypothesize an alternative transformation. The hypothesis has been effectively refuted,[13] and it has been shown that there is no fundamental contradiction between isothermal and nonisothermal kinetics. Nevertheless, the practical problem of inconsistency between Arrhenius parameters derived from isothermal and nonisothermal experiments persists today.

The discrepancies between Arrhenius parameters derived from isothermal and nonisothermal experiments arise form two main sources. The first is a result of commonly used methods of nonisothermal kinetic analysis that involve fitting of experimental data to assumed forms of the reaction model. Although there are examples[14,15] for which the use of model fitting of nonisothermal data resulted in Arrhenius parameters that are in reasonable agreement with values derived from isothermal data, generally this method fails to produce trustworthy kinetic

[⊗] Abstract published in *Advance ACS Abstracts,* October 1, 1997.

S1089-5639(97)01889-6 CCC: $14.00

TABLE 1: Set of Alternate Reaction Models Applied To Describe the Thermal Transformations in Solids

	reaction model	$f(\alpha)$	$g(\alpha)$
1	power law	$4\alpha^{3/4}$	$\alpha^{1/4}$
2	power law	$3\alpha^{2/3}$	$\alpha^{1/3}$
3	power law	$2\alpha^{1/2}$	$\alpha^{1/2}$
4	power law	$^2/_3\alpha^{-1/2}$	$\alpha^{3/2}$
5	one-dimensional diffusion	$^1/_2\alpha^{-1}$	α^2
6	Mampel (first order)	$1-\alpha$	$-\ln(1-\alpha)$
7	Avrami−Erofeev	$4(1-\alpha)[-\ln(1-\alpha)]^{3/4}$	$[-\ln(1-\alpha)]^{1/4}$
8	Avrami−Erofeev	$3(1-\alpha)[-\ln(1-\alpha)]^{2/3}$	$[-\ln(1-\alpha)]^{1/3}$
9	Avrami−Erofeev	$2(1-\alpha)[-\ln(1-\alpha)]^{1/2}$	$[-\ln(1-\alpha)]^{1/2}$
10	three-dimensional diffusion	$2(1-\alpha)^{2/3}(1-(1-\alpha)^{1/3})^{-1}$	$[1-(1-\alpha)^{1/3}]^2$
11	contracting sphere	$3(1-\alpha)^{2/3}$	$1-(1-\alpha)^{1/3}$
12	contracting cylinder	$2(1-\alpha)^{1/2}$	$1-(1-\alpha)^{1/2}$

information.[16] The model fitting methods do not achieve a clean separation between the temperature dependence, $k(T)$, and reaction model, $f(\alpha)$, which together describe the rate of reaction. The second major source of discrepancy arises from the fact that the temperature sensitivity of the reaction rate depends on the extent of conversion to products. This is partly a result of the inhomogeneous nature of solid state reactions; it also arises partly because many reactions follow complex mechanisms involving multiple series and parallel steps with different activation energies. Model fitting methods are designed to extract a single set of Arrhenius parameters for an overall process and are therefore unable to reveal this type of complexity in the rate expressions.

Isoconversional methods[17−19] are capable of addressing both of the aforementioned shortcomings of the model-fitting methods. Note that the method of Kissinger[20] that sometimes is assigned to the isoconversional methods, in our view, cannot be rightfully grouped with them because the value of T_m (the sample temperature at which the peak differential thermal analysis deflection occurs) used in this method corresponds to an extent of conversion that varies with the heating rate.[21] Techniques have been developed for extracting model-free estimates of the activation energy and preexponential factor,[22] as well as for numerical reconstruction of the reaction model.[23] Systematic studies of the variation in E with α that results from multistep mechanisms were started by Elder.[24] The ability of isoconversional methods to reveal this type of reaction complexity is therefore a crucial step toward the ability to draw mechanistic conclusions from kinetic data.[23] Although the method was successfully used[25−27] to analyze complex kinetics under both isothermal and nonisothermal conditions, it has not gained widespread acceptance.

In this paper, we present kinetic analyses of thermal decomposition data for ammonium dinitramide (ADN) by model fitting and isoconversional techniques. Because there is no set of Arrhenius parameters for this system that is generally accepted to be "correct", we have focused our attention on investigating the consistency between results derived from isothermal and nonisothermal experiments.

Experimental Section

A sample of ADN was kindly supplied by the Thiokol Corp. and was used without further purification. It was stored in darkness to prevent photochemical decomposition. The sample contains as much as 3% ammonium nitrate impurity, as determined by comparison of the measured melting point,[28] 92 °C, with the literature value.[29]

The thermogravimetric analysis (TGA) experiments were carried out using a Rheometrics Model 1000M TGA instrument. To reduce thermal gradients and exothermic self-heating, the experiments were performed on small (∼0.6 mg) samples. The sample temperature, which is controlled by a thermocouple, did not exhibit any systematic deviation from the preset linear temperature programs. Samples of ADN were placed in aluminum pans and heated in a flowing atmosphere of nitrogen (100 mL min^{-1}). For experiments carried out under nonisothermal conditions, the instrument was programmed to heat the sample from room temperature at a constant heating rate. After an initial period of nonlinear heating (<5 min), the programmed linear heating rates were established. The actual heating rates used in the kinetic analysis were calculated from temperature measurements made during the period of ADN decomposition.

For isothermal experiments, the temperature program was optimized to reach the preset isothermal temperature within 1.5 min without overshooting. During the next 1.5 min, the sample temperature was regulated to within ±1 °C of the set point. For the remainder of each run, the sample temperature was maintained within ±0.05 °C.

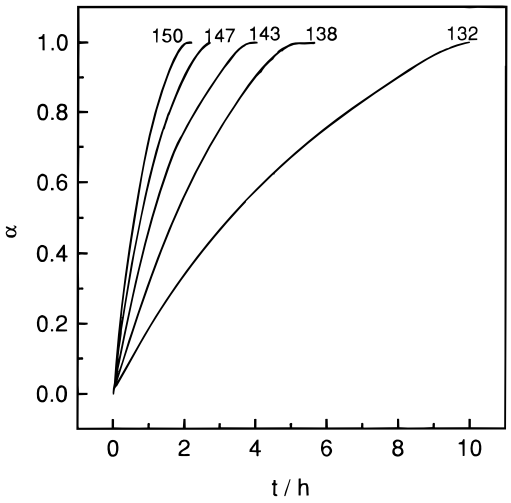

Figure 1. Thermogravimetric data showing the extent of ADN conversion during isothermal decomposition. The temperature of each experiment (in °C) is indicated by each curve.

Results

Kinetic curves showing the extent of reaction (fraction of the initial sample mass converted to gas-phase products) for experiments carried out under isothermal conditions are shown in Figure 1. These experiments were conducted at 132, 138, 143, 147, and 150 °C. The highest temperature (150 °C) of the isothermal experiments was chosen so that the extent of conversion did not exceed 1% during the first 1.5 min. In all cases, the samples were completely vaporized, and no residue remained in the aluminum sample pans at the conclusion of the run.

Nonisothermal runs were performed at constant heating rates of 1.5, 4.0, 5.5, 8.0, and 9.5 °C min^{-1}. These results are shown in Figure 2. It is noteworthy that the nonisothermal experiments cover a much wider range of temperatures than the isothermal

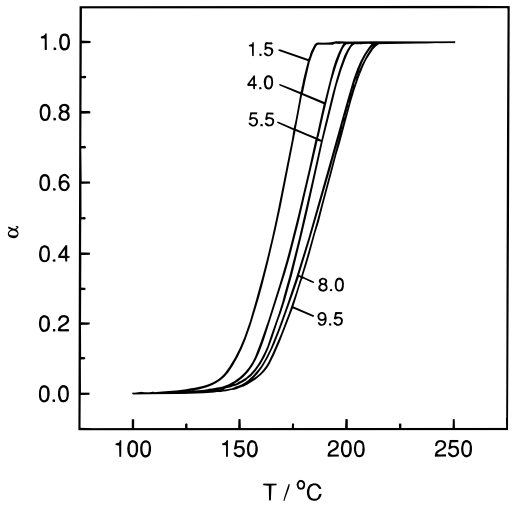

Figure 2. Thermogravimetric data showing the extent of ADN conversion during nonisothermal decomposition. The heating rate of each experiment (in °C min^{-1}) is indicated by each curve.

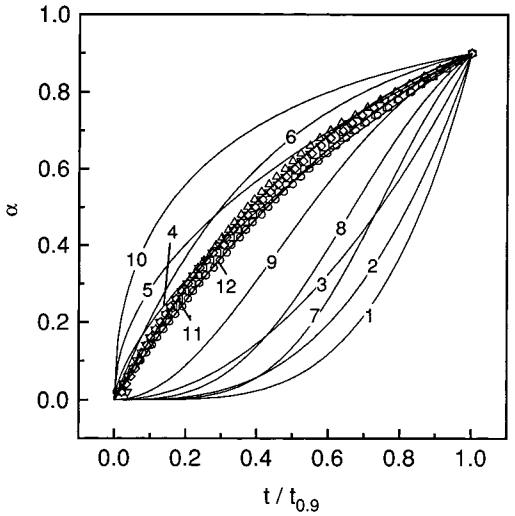

Figure 3. Reduced time plots for the reaction models (solid curves, as enumerated in Table 1) and isothermal experimental data for ADN decomposition at 150 °C (diamonds), 147 °C (down triangles), 143 °C (up triangles), 138 °C (circles), and 132 °C (squares).

experiments. The run at 1.5 °C min^{-1} covers a range of about 125−180 °C, whereas the 9.5 °C min^{-1} run covers about 140−220 °C.

Kinetic Computations

Model-Fitting Method. Rearrangement and integration of eq 1 for isothermal conditions gives

$$g_j(\alpha) = k_j(T)t \tag{4}$$

where $g(\alpha) = \int_0^\alpha [f(\alpha)]^{-1}\, d\alpha$ is the integrated form of the reaction model (Table 1). The subscript j has been introduced to emphasize that substituting a particular reaction model into eq 4 results in evaluating the corresponding rate constant, which is found from the slope of a plot of $g_j(\alpha)$ versus t. One method of choosing an appropriate reaction model is to plot α as a function of a reduced time variable t/t_α, where t_α is the time required to reach a specified conversion (e.g., 90% conversion). This method of kinetic analysis was first used by Letort[30] to determine reaction orders of homogeneous reactions. Later, it was used for more complex solid-state kinetics.[10,11,31] This is shown in Figure 3 for the experimental data obtained under isothermal conditions. For each reaction model selected, the rate constants are evaluated at several temperatures, T_i, and the Arrhenius parameters are evaluated in the usual manner using the Arrhenius equation in its logarithmic form,

$$\ln k_j(T_i) = \ln A_j - E_j/RT_i \tag{5}$$

Arrhenius parameters evaluated for the isothermal experimental data by the model-fitting method are presented in Table 2.

TABLE 2: Arrhenius Parameters for Isothermal Decomposition of ADN

model[a]	E/kJ mol^{-1}	ln(A/min^{-1})	$-r$
1	126.0	26.3	0.9949
2	126.1	26.6	0.9950
3	126.4	26.9	0.9952
4	127.7	27.6	0.9960
5	128.2	27.7	0.9963
6	129.5	29.2	0.9965
7	127.4	27.3	0.9956
8	127.6	27.6	0.9958
9	128.1	28.1	0.9960
10	130.3	27.4	0.9968
11	128.4	27.4	0.9962
12	128.1	27.5	0.9961

[a] Enumeration of the models is given in Table 1.

TABLE 3: Arrhenius Parameters for Nonisothermal Decomposition of ADN at 5.5 °C min^{-1}

model[a]	E/kJ mol^{-1}	ln(A/min^{-1})	$-r$
1	24.5	3.9	0.9783
2	35.1	6.9	0.9813
3	56.2	12.7	0.9837
4	182.9	46.2	0.9862
5	246.2	62.8	0.9865
6	139.4	35.7	0.9928[b]
7	29.5	5.3	0.9903
8	41.7	9.0	0.9913
9	66.1	15.9	0.9921[b]
10	269.1	67.4	0.9928[b]
11	131.0	32.0	0.9924[b]
12	127.6	31.3	0.9910

[a] Enumeration of the models is given in Table 1. [b] One of the four best, statistically equivalent models.

For nonisothermal conditions there are several relationships used to compute Arrhenius parameters,[13,31] each of which is based on an approximate form of the temperature integral that results from rearrangement and integration of eq 3

$$g(\alpha) = \frac{A}{\beta}\int_0^{T_\alpha} \exp\left(\frac{-E}{RT}\right) dT = \frac{I(E,T_\alpha)}{\beta} \tag{6}$$

One such approximation gives rise to the Coats−Redfern equation[32]

$$\ln[g_j(\alpha)/T^2] = \ln[(A_jR/\beta E_j)(1 - 2RT'/E_j)] - E_j/RT \tag{7}$$

where T' is the mean experimental temperature. This method is reported[33] to be one of the most frequently used to process nonisothermal data. Inserting various $g_j(\alpha)$ into eq 7 results in a set of Arrhenius parameters. A single pair of E and ln A is usually chosen as that corresponding to a reaction model that provides the best linearity of the plot $\ln[g_j(\alpha)/T^2]$ against T^{-1}. The Arrhenius parameters determined from the nonisothermal experimental data on ADN using this method are presented in Table 3.

Isoconversional Method. The basic assumption of the isoconversional method is that the reaction model, as defined in eq 1, is not dependent on temperature or heating rate. Under isothermal conditions, we may combine eq 4 and 5 to obtain

$$-\ln t_{\alpha,i} = \ln[A/g(\alpha)] - E_\alpha/RT_i \quad (8)$$

where E_α is evaluated from the slope of the plot $-\ln t_{\alpha,i}$ against T_i^{-1}.

For nonisothermal experiments, a nonlinear isoconversional method has been developed[34] which avoids inaccuracies associated with analytical approximations of the temperature integral. Because $g(\alpha)$ is independent of the heating rate, for any two experiments conducted at different heating rates, the ratio of the temperature integral $I(E,T_\alpha)$ to the heating rate β is a constant, as shown by eq 6. For a set of n experiments carried out at different heating rates, the activation energy can be determined at any particular value of α by finding the value of E_α for which the function

$$\sum_{i=1}^{n}\sum_{j\neq i}^{n}\frac{I(E_\alpha,T_{\alpha,i})\beta_j}{I(E_\alpha,T_{\alpha,i})\beta_i} \quad (9)$$

is a minimum. The minimization procedure is repeated for each value of α to find the dependence of activation energy on the extent of conversion. The nonisothermal experimental data shown in Figure 2 were processed using this procedure.

Discussion

Model Fitting Method. Examination of Table 2 shows that the Arrhenius parameters determined for the isothermal data using the model fitting method are almost independent of the reaction model. Analysis of reduced time plots for isothermal data (Figure 3) suggests that, of the reaction models shown in Table 1, the contracting sphere and contracting cylinder models provide the best fits to experimental data. These two models describe quite similar mechanisms and give rise to practically identical pairs of Arrhenius parameters. Therefore, the model fitting method works quite well in this case.

In contrast, the Arrhenius parameters obtained for nonisothermal decomposition of ADN are highly variable, exhibiting a strong dependence on the reaction model chosen (Table 3). Statistical analysis[35] of the linear correlation coefficients (r in Table 3) can identify the four "best" reaction models, which in this example are statistically equivalent. Although model 11 (contracting sphere) is one of the four best, there is nothing about the model fitting analysis to indicate that it is any better or worse than the other three "best fit" models (models 6, 9, or 10). The four models describe absolutely different mechanisms, and the corresponding Arrhenius parameters span a factor of 4 in activation energy and ln A. Clearly, the model fitting method gives highly uncertain Arrhenius parameters for nonisothermal data and therefore cannot be used to make a meaningful comparison of isothermal and nonisothermal experiments.

The reason for the failure of the model fitting method, as applied to nonisothermal data, is clear. Unlike the isothermal experiments, in which temperature is isolated as an experimental variable, the nonisothermal experiments allow fits that vary the temperature sensitivity (E, ln A) and reaction model $f(\alpha)$, simultaneously. In many cases, this extra flexibility in the fitting procedure allows errors in the functional form of the reaction model to be concealed by making compensating errors in the Arrhenius parameters, sometimes by as much as 1 order of magnitude.[26,36−38] Because the experiments are typically carried out over a relatively narrow range of temperatures, this kinetic compensation effect usually prevents a reliable determination of the Arrhenius parameters and reaction model from nonisothermal data using the model fitting method.[39] A review[16] has highlighted some of the more spectacular failures of the model fitting method as applied to nonisothermal experimental data.[40−45] These problems have led some researchers to mistrust kinetic results of nonisothermal experiments in general;[46] however, in our view this attitude is justifiable only as it pertains to the use of the model fitting method. Given a proper kinetic treatment, nonisothermal experiments are unquestionably capable of producing reliable kinetic information.[16]

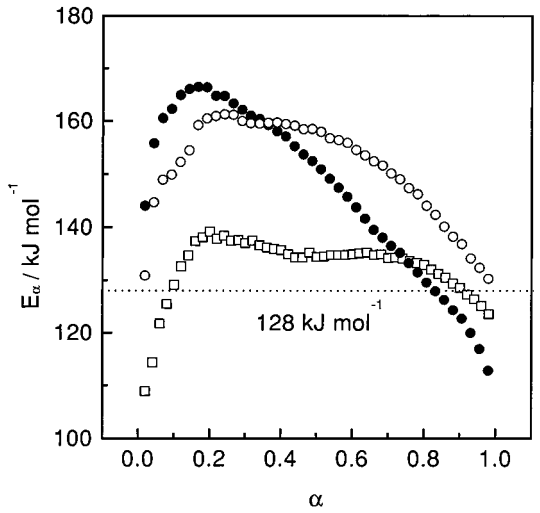

Figure 4. Dependencies of the activation energy on extent of conversion determined using the model-free isoconversional technique for the isothermal data (open squares) and nonisothermal data (open circles: β = 1.5, 4.0, and 5.5 °C min^{-1}; solid circles: β = 1.5, 4.0, 5.5, 8.0, and 9.5 °C min^{-1}). The dashed line represents the value obtained by the model fitting method from isothermal data.

Isoconversional Method. Application of eq 8 to the isothermal data for ADN decomposition permits a determination of E_α as a function of α. This is shown by the open squares in Figure 4. The activation energy rises from about 110 kJ mol^{-1} at low conversion to nearly 140 kJ mol^{-1} at 20% conversion, and it subsequently decreases to about 124 kJ mol^{-1} near the completion of the reaction. Unlike the model fitting method, which yields a single overall value of activation energy for the process (128 kJ mol^{-1} in this case), the isoconversional technique may reveal complexity of the reaction mechanism in the form of a functional dependence of the activation energy on the extent of conversion. Because most solid-state reactions are not simple one-step processes, analysis of isothermal data by the isoconversional technique is well-suited to revealing this type of complexity that might be disguised in the model fitting kinetic analysis (cf. Figure 4).

Figure 4 shows the dependence of the activation energy on extent of ADN conversion, as computed by the nonlinear isoconversional method (vide supra). The dependence is similar in shape to the isothermal one. When all five data sets are included in the analysis (solid circles in Figure 4), the activation energy increases to a maximum around 168 kJ mol^{-1} at 17% conversion and then decreases monotonically to 112 kJ mol^{-1} near the end of the reaction. When only the results of the experiments at the three lowest heating rates are included, the variation in E_α is not as dramatic. This behavior may be indicative of a multistep reaction mechanism in which an early step in the mechanism having a high activation energy can dominate the kinetics at faster heating rates, due the higher temperatures reached in that type of experiment.

Whereas the isothermal and nonisothermal dependencies of E_α on α have rather similar shapes, their direct comparison should not be made because the nonisothermal experiments cover a much wider range of temperatures (125−220 °C) than is practical for the isothermal experiments (132−150 °C). The use of slow heating rates allows one to narrow the temperature region of a nonisothermal experiment. This may help to reduce the quantitative difference between the dependencies of E_α on

α derived for isothermal and nonisothermal experiments (Figure 4). However, significant differences between the results of isothermal and nonisothermal experiments may persist. We decided to examine this point more closely in the following section.

Analysis of Synthetic Data for a Model Reaction System

Analysis of experimental data is advantageous from the standpoint of being firmly grounded in reality; however, comparison of isothermal and nonisothermal results can be marred by some uncontrolled experimental factors, such as as mass and thermal transport, the temperature jump required to start each isothermal experiment, and others. For this reason, we decided to consider an ideal case of synthetic data generated by numerical simulation of a model reaction system. The particular kinetic scheme chosen is two parallel reaction channels,

$$\mathrm{A} \rightarrow \text{products} \tag{10a}$$

$$\mathrm{B} \rightarrow \text{products} \tag{10b}$$

each of which follows Mampel's (first-order) model. This model is the most widely used[47] of the models given in Table 1 and is rooted in the basic concepts of solid-state reactions.[48] The chosen reaction system is appropriate for a mixture of two different solids that react in the same temperature region[49] or reaction of a mixture of isomers.[50−52] The model may also be appropriate for a system in which localized melting causes reaction to occur in both the liquid and solid phases.[53]

Assuming that the two channels make equal contributions to α, the overall reaction rate is

$$\frac{\mathrm{d}\alpha}{\mathrm{d}t} = \left(\frac{\mathrm{d}\alpha_1}{\mathrm{d}t} + \frac{\mathrm{d}\alpha_2}{\mathrm{d}t}\right) = \frac{1}{2}[k_1(T)(1-\alpha_1) + k_2(T)(1-\alpha_2)] \tag{11}$$

The effective activation energy of the process is

$$E_\alpha = \left[\frac{\mathrm{d}\ln(\mathrm{d}\alpha/\mathrm{d}t)}{\mathrm{d}T^{-1}}\right]_\alpha = \frac{E_1 k_1(T)(1-\alpha_1) + E_2 k_2(T)(1-\alpha_2)}{k_1(T)(1-\alpha_1) + k_2(T)(1-\alpha_2)} \tag{12}$$

which is clearly a function of both temperature and extent of conversion.

The Arrhenius parameters of individual steps were taken to be $A_1 = 10^{10}$ min^{-1}, $E_1 = 80$ kJ mol^{-1} and $A_2 = 10^{15}$ min^{-1}, $E_2 = 120$ kJ mol^{-1}. These values were chosen so that the rates of the two steps are comparable within the working range of temperatures. A total of 41 isothermal simulations were performed, spanning the range 320−480 K in steps of 4 K. At each temperature, we determined the values of α_1 and α_2 corresponding to overall conversions $0.01 \leqslant \alpha \leqslant 0.99$ in intervals of 0.02. The values of T, α_1, and α_2 were substituted into eq 12 to plot the effective activation energy as a function of the temperature and overall conversion for isothermal conditions. The results are shown in Figure 5.

Fifty nonisothermal simulations were also performed to cover the experimentally practicable range of heating rates from 0.5 to 100 K min^{-1}. The temperature integral was computed using the approximation of Senum and Yang.[54] For each simulation, 50 temperatures were determined corresponding to extents of overall conversion $0.01 \leqslant \alpha \leqslant 0.99$ in intervals of 0.02. These temperatures and the corresponding partial conversions α_1 and α_2 were inserted into eq 12 to plot the effective activation energy as a function of the temperature and overall conversion. The

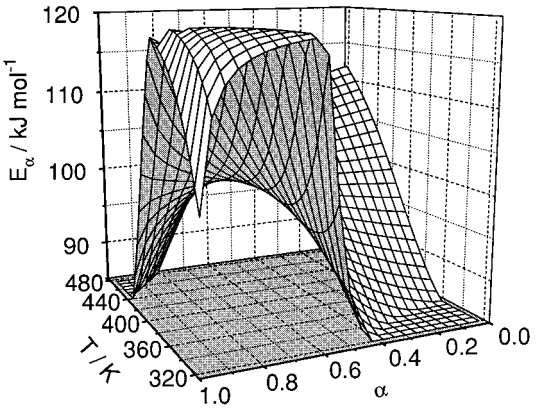

Figure 5. Surface plot of activation energy as a function of extent of conversion and temperature for synthetically generated data under isothermal conditions.

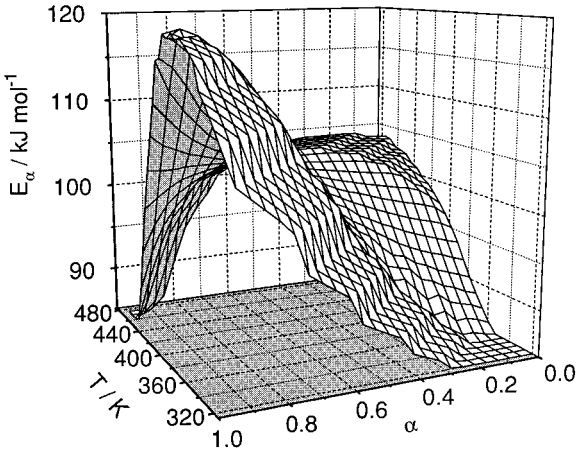

Figure 6. Surface plot of activation energy as a function of extent of conversion and temperature for synthetically generated data under nonisothermal conditions.

temperature region covered in the nonisothermal simulations was approximately 320 K ($T_{0.01}$ at 0.5 K min^{-1}) to 480 K ($T_{0.99}$ at 100 K min^{-1}). The resulting surface plot of E_α as a function of T and α for nonisothermal simulations is shown in Figure 6.

Although the surfaces presented in Figures 5 and 6 have some common features (the same locations of minima, rather close locations of the maximum, and the range of variation in E_α), the shapes of the surfaces are different. The root cause is that the global extent of conversion (α) does not uniquely determine the composition of the sample (α_1, α_2). At the same values of α and T, the contributions of the single reaction measured as α_1 and α_2 are respectively different in the isothermal and nonisothermal experiment. This ultimately causes the surfaces in Figures 5 and 6 to have different shapes.

Whereas synthetic data allow E_α to be determined at any single temperature, experimental evaluation of E_α requires several experiments to be performed at different temperatures or heating rates. For this reason, experimentally determined dependencies of E_α on α are always averaged over some temperature interval. The activation energy derived from isothermal experiments is an average over the range of temperatures selected for the experiments, whereas the E_α derived from nonisothermal experiments is an average over a variable range of rising temperatures. Therefore, isothermal and nonisothermal experiments not only give rise to different $E(\alpha,T)$ surfaces, but they also cut and average slices of these surfaces in different ways. The upshot is that we may not generally expect that the isothermal and nonisothermal dependencies of E_α on α that we observe as the projections of those cuts to be identical. However, because of the aforementioned common

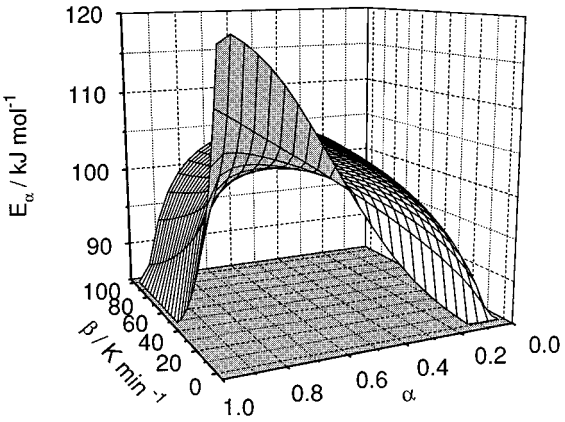

Figure 7. Surface plot of activation energy as a function of extent of conversion and heating rate for synthetically generated data under nonisothermal conditions.

features of the isothermal and nonisothermal surfaces, we may expect that under certain conditions the corresponding dependencies of E_α on α will be quite similar. By conducting the experiments over comparable ranges of temperature, we may bring the isothermal and nonisothermal dependencies of E_α on α closer to each other. However, it is difficult to conduct isothermal experiments over a wide range of temperatures. For instance, isothermal experiments can hardly be conducted in the temperature region 320−480 K. The time to completion of the process is about 10 s at 480 K and more than 2 months at 320 K. Practical temperatures region would rather be 360−400 K with respective times to completion 1000−20 min. Variation of the heating rate allows for significant changes in the temperature region of a nonisothermal experiment. An increase of the heating rate from 0.5 to 100 K min^{-1} makes the temperature region ($T_{0.01}-T_{0.99}$) of the experiment change from 320−400 to 390−480 K. Variation of the heating rate is thus an effective means of manipulating the dependence of E_α on α. Figure 7 presents the surface of the effective activation energy as a function of α and β. As seen in this figure, the E_a dependencies at slow heating rates (<10 K min^{-1}) show reasonable similarity to the E_α dependence at the temperatures accessible in the isothermal experiments (Figure 5). The experimental data for thermal decomposition of ADN (cf. Figure 4) appear to support this conclusion.

Conclusions

The model fitting kinetic analysis applied to nonisothermal data produces Arrhenius parameters that are so uncertain that they cannot be meaningfully compared with the isothermal values. The application of the model fitting technique to isothermal data gives rise to unambiguous values of Arrhenius parameters that may, however, conceal complex (e.g., multistep) kinetics. A viable alternative to the model fitting method is the model-free isoconversional method. When applied to nonisothermal data, this method allows one to obtain unambiguous values of Arrhenius parameters. For isothermal data, the use of the isoconversional method is an effective means of unmasking complex kinetics. Because it is applicable to both isothermal and nonisothermal data, the isoconversional method represents a way toward consistent kinetic results. On the basis of synthetic and experimental data obtained under both isothermal and nonisothermal conditions, we have shown that the isoconversional method is capable of producing similar E_α dependencies which, however, are unlikely to be identical. The quantitative consistency of E_α dependencies can be improved by bringing the temperature regions of isothermal and nonisothermal experiments closer to each other.

Acknowledgment. This work is supported by the Office of Naval Research and Program Officer Dr. Richard S. Miller through Contract N00014-95-1-1339.

References and Notes

(1) Jost, W. *Diffusion und Chemische Reaktionen in Festen Stoffen*; T. Steinkopff: Dresden, Leipzig, 1937.
(2) Hedwall, J. A. *Reaktionsfahigkeit Festen Stoffe*; J. A. Barth: Leipzig, 1938.
(3) *Chemistry of the Solid State*; Garner, W. E., Ed.; Butterworth: London, 1955.
(4) Garn, P. D. *Crit. Rev. Anal. Chem.*, **1972,** *4*, 65.
(5) Garn, P. D. *Thermochim. Acta* **1990**, *160*, 135.
(6) Raghavan, V.; Cohen, M. In *Treatise of Solid State Chemistry*; Plenum Press: New York, 1975; Vol. 5, p 67.
(7) Le Claire, A. D. In *Treatise of Solid State Chemistry*; Plenum Press: New York, 1975; Vol. 4, p 1.
(8) Galwey, A. K.; Brown, M. E. *Proc. R. Soc. London A* **1995**, *450*, 501.
(9) Maciejewski, M. *J. Therm. Anal.* **1992**, *38*, 51.
(10) Delmon, B. *Introdition a la Cinetique Heterogene*; Editions Technip: Paris, 1969.
(11) Barret, P. *Cinetique Heterogene*; Gauthier-Villars: Paris, 1973.
(12) McCallum, J. R.; Tanner, J. *Nature* **1970,** *225*, 1127.
(13) Sestak, J. *Thermophysical Properties of Solids. Comprehensive Analytical Chemistry*; Elsevier: Amsterdam, 1984; Vol. 12D.
(14) Johnson, D. W.; Gallagher, P. K. *J. Phys. Chem.* **1972**, *76*, 1474.
(15) Gallagher, P. K.; Johnson, D. W. *Thermochim. Acta* **1973**, *6*, 67.
(16) Vyazovkin, S.; Wight, C. A. *Annu. Rev. Phys. Chem.* **1997**, *48*, 119.
(17) Friedman, H. *J. Polym. Sci.* **1963**, *6C*, 183.
(18) Ozawa, T. *Bull. Chem. Soc. Jpn.* **1965**, *38*, 1881.
(19) Flynn, J. H.; Wall, L. A. *J. Res. Natl. Bur. Stand.* **1996**, *70A*, 487.
(20) Kissinger, H. E. *Anal. Chem.* **1957**, *29*, 1702.
(21) Tang, T. B.; Chaudhri, M. M. *J. Therm. Anal.* **1980**, *18*, 247.
(22) Vyazovkin, S.; Linert, W. *Chem. Phys.* **1995**, *193*, 109.
(23) Vyazovkin, S. *Int. J. Chem. Kinet.* **1996**, *28*, 95.
(24) Elder, J. P. *J. Therm. Anal.* **1984**, *29*, 1327.
(25) Huang, J.; Gallagher, P. K. *Thermochim. Acta* **1991**, *192*, 35.
(26) Tanaka, H.; Koga, N.; Sestak, J. *Thermochim. Acta* **1992**, *203*, 203.
(27) Vyazovkin, S.; Sbirrazzuoli, N. *Macromolecules* **1996**, *29*, 1867.
(28) Vyazovkin, S.; Wight, C. A. *J. Phys. Chem. A* **1997**, *101*, 5653.
(29) Russell, T. P.; Piermarini, G. J.; Block, S.; Miller, P. J. *J. Phys. Chem.* **1996**, *100*, 3248.
(30) Letort, M. J. *Chim. Phys.* **1937**, *34*, 206.
(31) Brown, M. E.; Dollimore, D.; Galwey, A. K. *Reactions in the Solid State. Comprehensive Chemical Kinetics*; Elsevier: Amsterdam, 1980; Vol. 22.
(32) Coats, A. W.; Redfern, J. P. *Nature* **1964**, *201*, 68.
(33) Carr, N. J.; Galwey, A. K. *Thermochim. Acta* **1984**, *79*, 323.
(34) Vyazovkin, S. *J. Comput. Chem.* **1997**, *18*, 393.
(35) Johnson, N. L.; Leone, F. C. *Statistics and Experimental Design in Engineering and the Physical Sciences*; John Wiley & Sons: New York, 1977.
(36) Li, J.; Zhang, G.; Wang, J. *Thermochim. Acta* **1992**, *207*, 219.
(37) Galwey, A. K.; Koga, N.; Tanaka, H. *J. Chem. Soc., Faraday Trans.* **1990**, *86*, 531.
(38) Tanaka, H.; Koga, N. *J. Phys. Chem.* **1988**, *92*, 7023.
(39) Brill, T. B.; Gongwer, P. E.; Williams, G. K. *J. Phys. Chem.* **1994**, *98*, 12242.
(40) Singh Raman, R. K.; Parida, F. C.; Khanna, A. S. *J. Therm. Anal.* **1988**, *34*, 1043.
(41) Gabr, R. M.; Girgis, M. M.; El-Awad, A. M. *Thermochim. Acta* **1992**, *196*, 279.
(42) Mallikarjun, K. G.; Naidu, R. S. *Thermochim. Acta* **1992**, *206*, 273.
(43) Zheng, L.; Dai, L.; Xin, X. *Thermochim. Acta* **1992**, *196*, 437.
(44) Abd El-Salam, K. M.; Halawani, K. H.; Fakiha1, S. A. *Thermochim. Acta* **1992**, *204*, 311.
(45) Sawney, S. S.; Chauhan, G. S.; Aslam, M. *Thermochim. Acta* **1992**, *204*, 321.
(46) Boldyreva, E. *Thermochim. Acta* **1987**, *110*, 107.
(47) Carr, N. J.; Galwey, A. K. *Thermochim. Acta* **1984**, *79*, 323.
(48) Mampel, K. L. *Z. Phys. Chem. (Munich)* **1940**, *187A*, 235.
(49) Berger, B.; Brammer, A. J.; Charsley, E. L. Book of Abstracts, 6th ESTAC, Grado, Italy, Sept 11−16, 1994; p 61.
(50) Shlensky, O. F.; Vaynsteyn, E. F.; Matyukhin, A. A. *J. Therm. Anal.* **1988**, *34*, 645.
(51) Levchik, S. V.; Bolvanovich, E. E.; Lesnikovich, A. I.; Ivashkevich, O. A.; Gaponik, P. N.; Vyazovkin, S. V. *Thermochim. Acta* **1990**, *168*, 211.
(52) Schneider, H. A. *J. Therm. Anal.* **1993**, *40*, 677.
(53) Galwey, A. K. *J. Therm. Anal.* **1994,** *41*, 267.
(54) Senum, G. I.; Yang, R. T. *J. Therm. Anal.* **1979**, *11*, 445.